

Direct laser acceleration of electrons by tightly focused laser pulses.

Tianhong Wang¹, Vladimir Khudik^{1,2}, Alexey Arefiev³ and Gennady Shvets¹

¹*School of Applied and Engineering Physics, Cornell University, Ithaca, New York 14850, USA.*

²*Department of Physics and Institute for Fusion Studies,*

The University of Texas at Austin, Austin, Texas 78712, USA.

³*Department of Mechanical Engineering and Center for Energy Research,
University of California, San Diego, California 92093, USA.*

(Dated: December 14, 2018)

We present an analytical theory that reveals the importance of the longitudinal laser electric field in the resonant acceleration of relativistic electrons by the tightly confined laser beam. It is shown that this field always counterworks to the laser transverse component and effectively decreases the final energy gain of electrons through direct laser acceleration mechanism. This effect is demonstrated by carrying out the particle-in-cell simulations in the setup where the wakefield in the plasma bubble is compensated by the longitudinal laser electric field experienced by the accelerated electrons. The derived scalings and estimates are in good agreement with numerical simulations.

PACS numbers:

I. INTRODUCTION

As high intensity ($> 10^{18} \text{W/cm}^{-2}$) laser beams propagate in an underdense plasma, their radiation pressure expels electrons out of the propagation path. Long beam (with pulse duration τ much longer than ω_p^{-1} , where $\omega_p = \sqrt{4\pi e^2 n/m_e}$ is the plasma frequency, n is the plasma density, m_e is the electron mass, and $-e$ is the electron charge) can support slowly evolving quasistationary ion channels in which the longitudinal electric field is weak [1, 2]. The laser wave accelerates electrons oscillating across the channel to the energy much higher than the energy gained by free electrons in the vacuum [3]. This acceleration regime is interesting for potential applications of copious relativistic electrons as a compact X-ray sources [4–6], and novel sources of energetic ions [7], neutrons [8], and positrons [9].

Short beam ($\tau < \omega_p^{-1}$) generates an extremely nonlinear plasma wave blow-out structure known as a "plasma bubble" [10] in which strong longitudinal electric field is capable of accelerating electrons injected at the bottom of the bubble up to multi-GeV scale over short distance [11–14]. The laser pulse overlapping with relativistic electrons additionally boosts their energy through direct laser acceleration (DLA) mechanism [15]. Recently it has been shown that the relativistic electrons injected in the front portion of the plasma bubble in the decelerating phase of the plasma wave can also gain ultra-relativistic energy from the bubble-forming laser pulse through inverse ion-channel laser mechanism [16].

During direct laser acceleration, the laser electric field pumps energy into transverse (betatron) oscillation which is redirected by the magnetic field into the longitudinal momentum. The resonant interaction of electrons with high-intensity laser wave is complicated by the fact that the Doppler shifted frequency of the wave $\omega_D = \omega_L(1 - v_x/v_{ph})$, where ω_L is the wave frequency, v_{ph} is its phase velocity and v_x is the longitudinal particle velocity, only in average equals to the betatron fre-

quency $\omega_\beta = \omega_p/\sqrt{2\gamma}$ of the electron oscillations in the channel [17]. Strong non-linearity of the laser-particle interaction leads to an irregular (stochastic) motion of electrons in the ion channel [18] and high sensitivity of the gained energy to the initial conditions.

Since transverse laser wave fields are mainly responsible for DLA mechanism, DLA mechanism is analytically studied by approximating the laser pulse by a planar electromagnetic wave [19–24]. In this paper, we examine through an analytical theory and supporting PIC simulations the effect of a small but finite longitudinal electric field of the laser pulse in the DLA regime. It is shown that this field can produce a significant deceleration effect that partially offsets the resonant acceleration by the transverse component of tightly focused laser pulses.

The remainder of the paper is organized as follows. In Sec. II, we develop an analytical model by replicating the electromagnetic fields in the wave propagating in the ion channel. We find in Sec. III the scaling law for the work performed by the longitudinal component of the laser pulse. In Sec. IV we carry out particle-in-cell simulations of the resonant interaction of relativistic electrons with the DLA laser pulse in the plasma bubble generated by the leading (pump) pulse [25–27]. Summary of the work is presented in Sec. V.

II. MODEL

In order to capture the effect of laser longitudinal electric field, we consider a simplified setup which well approximates physics of the particle-wave interaction in the ion channels created by multi-picosecond laser beams, see Fig. 1.

The ion channel is modeled under the following assumptions: it is created in tenuous plasma by full evacuation of electrons from a cylinder of the finite radius $R \gg \lambda_L$, where λ_L is the laser wavelength. We neglect the slow evolution of the channel considering it as a qua-

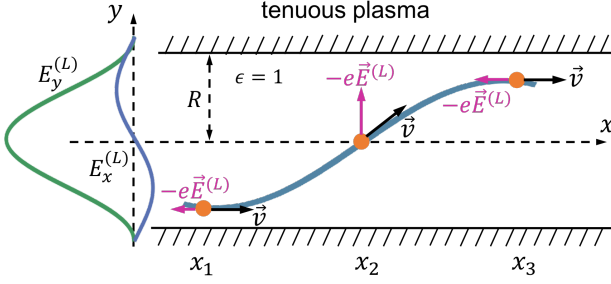


FIG. 1: Sketch of the electron motion and electric fields of the laser pulse propagating in the ion channel. The electron quickly gains energy when it resonantly interacts with the laser wave. The phases of transverse and longitudinal components of the electric field ($E_y^{(L)}$ and $E_x^{(L)}$) are shifted by $\pi/2$: $E_y^{(L)} = 0$ at the electron turning points x_1 and x_3 while $E_x^{(L)}$ has the same sign at these points.

sistationary formation [28].

The laser wave propagates in the x -direction aligned with the channel axis. It is linearly polarized in y -direction so that $E_y^{(L)}$ is the main component of the laser electric field. In the cylindrical channel, there are only two components of the electric field $E_y^{(L)}$, $E_x^{(L)}$ and one component of the magnetic field $B_z^{(L)}$ do not vanish in the main plane $x - y$ depicted in Fig. 1. The radial electrostatic field in the channel is approximated as $E_y = m\omega_p^2 y / 2e$. The dynamics of relativistic electrons is then described in this model by:

$$\frac{dp_x}{dt} = -eE_x^{(L)} - \frac{e}{c}v_y B_z^{(L)}, \quad (1)$$

$$\frac{dp_y}{dt} = -\frac{1}{2}m\omega_p^2 y - e\left(E_y^{(L)} - \frac{v_x}{c}B_z^{(L)}\right), \quad (2)$$

$$\frac{dx}{dt} = v_x = \frac{p_x}{m\gamma}, \quad \frac{dy}{dt} = v_y = \frac{p_y}{m\gamma} \quad (3)$$

where $\gamma = (1 + \mathbf{p}^2/m^2c^2)^{1/2}$ is the electron relativistic factor, and c is the speed of light. Compared with previous models, where the laser wave is considered to be planar, these equations contain the longitudinal component of the laser electric field which can profoundly impact the energy gain of resonantly accelerated electrons.

We assume that $E_y^{(L)} \propto \cos \phi$, where $\phi = \omega_L(x/v_{\text{ph}} - t) \equiv k_x x - \omega_L t$ is the phase of the laser wave, and $k_x = \omega_L/v_{\text{ph}}$ is the x -component of the laser wavenumber. Since heavy ions in the channel are considered to be immobile, this field satisfies the wave equation in the vacuum:

$$\nabla_{\perp}^2 E_y^{(L)} = -k_{\perp}^2 E_y^{(L)}. \quad (4)$$

where $k_{\perp} = \sqrt{k_L^2 - k_x^2}$ and $k_L = \omega_L/c$.

The z -component of the electric field does not vanish in the $y - z$ plane and can be estimated in the tenuous plasma as $E_z^{(L)} \lesssim (\omega_p/\omega_L)^2 E_y^{(L)} \ll E_y^{(L)}$. Then, the lon-

gitudinal component $E_x^{(L)}$ is found from Poisson equation

$$\frac{\partial E_x^{(L)}}{\partial x} + \frac{\partial E_y^{(L)}}{\partial y} = 0, \quad (5)$$

in which a small term $\partial E_z^{(L)}/\partial z \ll \partial E_y^{(L)}/\partial y$ is omitted, and the z -component of the magnetic field is found from the Ampere-Maxwell equation

$$-\frac{1}{c} \frac{\partial B_z^{(L)}}{\partial t} = \frac{\partial E_y^{(L)}}{\partial x} - \frac{\partial E_x^{(L)}}{\partial y}. \quad (6)$$

The solution of Eqs. (4) - (6) for the linearly polarized laser wave is given by

$$E_y^{(L)} = E_0 J_0(k_{\perp} y) \cos \phi, \quad (7)$$

$$E_x^{(L)} = \frac{k_{\perp}}{k_x} E_0 J_1(k_{\perp} y) \sin \phi, \quad (8)$$

$$B_z^{(L)} = \frac{c}{v_{\text{ph}}} E_0 \left[J_0(k_{\perp} y) + \frac{k_{\perp}^2}{k_x^2} J_1'(k_{\perp} y) \right] \cos \phi, \quad (9)$$

where $E_0 = a_0(m c \omega_L / e)$ is the amplitude of the laser electric field, a_0 is the dimensionless amplitude of the vector potential, $J_0(\xi)$ and $J_1(\xi)$ are Bessel functions of the first kind and $J_1'(\xi) \equiv dJ_1(\xi)/d\xi$.

The transverse wavenumber k_{\perp} for fundamental mode of the linearly polarized laser wave [29] can be estimated by setting outside the channel the main component of the electric field (7) to zero:

$$J_0(k_{\perp} R_*) = 0, \quad k_{\perp} \approx 2.4/R_*, \quad (10)$$

where $R_* \equiv R + \delta_s$ and $\delta_s = c/\omega_p$ is accounted for the finite skin depth. Then we estimate $k_x = (k_L^2 - k_{\perp}^2)^{1/2} \approx k_L [1 - 2.88/(k_L^2 R_*^2)]$ and

$$v_{\text{ph}} \approx c [1 + 2.88/(k_L^2 R_*^2)]. \quad (11)$$

Equations (1) - (3) complemented by the expressions for fields (7) - (9) fully determine relativistic dynamics of electrons under action of the laser wave confined in the ion channel.

Typical energy gain during particle-wave resonant interaction is shown in Fig. 2. First noteworthy feature of such an interaction is that the different components of the laser electric field work in opposite way: while $E_y^{(L)}$ pumps energy into electron oscillations effectively accelerating particle, $E_x^{(L)}$ returns part of this energy to the laser wave decreasing the resulting energy gain, see Fig. 2(a). The other striking feature is that although the longitudinal component is much less than the transverse one [$E_x^{(L)}/E_y^{(L)} \sim 1/60$ in Fig. 2(b)], the corresponding longitudinal and transverse works are not so different: $|W_{\parallel}|/W_{\perp} \sim 1/5$ (and $|W_{\parallel}|/m c^2 \gamma \sim 1/4$).

III. RESONANT DLA IN ION CHANNELS

In this section, we examine the motion of relativistic electrons governed by Eqs. (1) - (3) and derive an

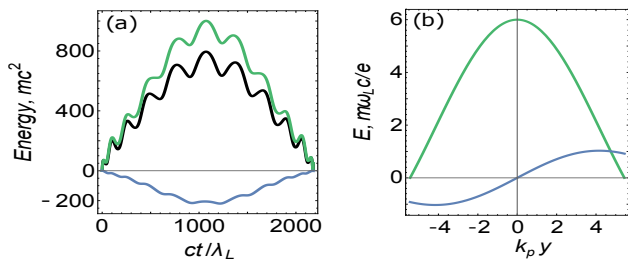


FIG. 2: The energy gain of electron resonantly interacting with the laser wave confined in the ion channel. (a) The time dependence of the electron energy (black) and the works performed by the transverse and longitudinal laser fields (green and blue, respectively). The electron is initially placed at rest on the channel axis at $\phi|_{t=0} = \frac{\pi}{2}$. The laser-plasma parameters are: $a_0 = 6$, $\omega_p/\omega_L = 1/15$, $k_p R_* \approx 5.44$. (b) Transverse and longitudinal laser fields in the ion channel: $E_y^{(L)}(y)$ (brown) and $10 \times E_x^{(L)}(y)$ (blue); the phase of these fields is shifted by $\pi/2$.

analytical expression for the work done by longitudinal component of the laser beam.

A. Phase coupling

We start our analysis by noting that Hamiltonian H of particle motion depends on x and t only through combination $x - v_{\text{ph}}t$, and hence $H - v_{\text{ph}}P_x$, where P_x is the x -component of the canonical momentum, is conserved. Therefore, equations (1) - (3) have the following integral of motion:

$$\gamma - \frac{v_{\text{ph}}}{c} \left(\frac{p_x}{mc} - a_x \right) + \frac{1}{4} k_p^2 y^2 = I_0 = \text{const}, \quad (12)$$

where $a_x = -(k_{\perp}/k_x) a_0 J_1(k_{\perp} y) \cos \phi$ is the x -component of the dimensionless vector potential of the laser wave, and the constant I_0 is determined by the initial position and momentum of the particle. Equation (12) can be simplified for the luminal wave ($v_{\text{ph}} = c$) and electrons moving with relativistic speed along channel axis ($p_x \gg p_y \gg 1$)

$$\frac{1}{2c^2} \gamma v_y^2 + \frac{1}{4} k_p^2 y^2 = I_0 - a_x, \quad (13)$$

Assuming that $I_0 \gg a_x$, we find that $y \approx 2(I_0)^{1/2} k_p^{-1} \sin \psi$, $v_y \approx c(2I_0/\gamma)^{1/2} \cos \psi$, and $d\psi/dt \equiv \omega_{\beta} = \omega_p/(2\gamma)^{1/2}$, where ψ is the phase of betatron oscillations. In this regime the time-derivative of the wave phase can be expressed in terms of the phase of betatron oscillations: $d\phi/dt = -\omega_D$, where $\omega_D = \omega_L(1 - v_x/c) \approx \omega_L(1 - v_x^2/c^2)/2 \approx \omega_L v_y^2/2c^2 = \omega_L(I_0/\gamma) \cos^2 \psi$. Assuming that change of the relativistic factor is small during one betatron period, we can find that $d\phi/d\psi = -2(\omega_D/\omega_{\beta}) \cos^2 \psi$ and hence the wave phase and the phase of betatron oscillations of the relativistic electron

are coupled by the relation

$$\phi = \theta - (\langle \omega_D \rangle / \omega_{\beta}) \left(\psi + \frac{1}{2} \sin 2\psi \right), \quad (14)$$

where θ is the phase mismatch which approximately constant during one betatron oscillation, and $\langle \omega_D \rangle = \omega_L/(2I_0\gamma)$.

B. Scaling law

The relationship between the longitudinal and transverse works, W_{\parallel} and W_{\perp} , and the relativistic factor γ during resonant interaction of relativistic electrons co-propagating with laser wave in the ion channel can be easily found for small amplitude of betatron oscillations. In this case the components of the laser electric field can be approximated as $E_x \approx \frac{1}{2}(k_{\perp}/k_x) k_{\perp} y E_0 \sin \phi$ and $E_y^{(L)} \approx E_0 \cos \phi$. Then expressions for corresponding works (normalized to mc^2) take the following form:

$$\frac{dW_{\parallel}}{dt} = -\frac{eE_x^{(L)}v_x}{mc^2} \approx -eE_0c \frac{k_{\perp}^2}{k_L k_p} I_0^{1/2} \sin \phi \sin \psi, \quad (15)$$

$$\frac{dW_{\perp}}{dt} = -\frac{eE_y^{(L)}v_y}{mc^2} \approx -eE_0c \sqrt{\frac{2}{\gamma}} I_0^{1/2} \cos \phi \cos \psi, \quad (16)$$

Assuming that γ is approximately constant during one betatron period, we can use Eq. (14) to average the trigonometric functions in r.h.s. of Eqs. (15) and (16) over betatron oscillations. The result is especially simple near the resonance $\omega_{\beta} \approx \langle \omega_D \rangle$ [30]: $\langle \sin \phi \sin \psi \rangle = \alpha_{\parallel} \cos \theta$ and $\langle \cos \phi \cos \psi \rangle = \alpha_{\perp} \cos \theta$, where $\alpha_{\parallel} = -0.59$ and $\alpha_{\perp} = 0.348$. Since α_{\parallel} is negative, the longitudinal component of the laser electric field always works in opposite way compared to the transverse component. Note that during the resonant motion depicted in Fig. 1, the phase mismatch is $\theta = -\pi$, and phases of the betatron oscillations and laser wave at the position $x = x_1$ are $\psi|_{x=x_1} = \phi|_{x=x_1} = -\frac{\pi}{2}$.

For sake of simplicity, we neglect the change of the numerical factors α_{\parallel} and α_{\perp} caused by the detuning from the resonance. Then we reduce averaged Eqs. (15) and (16) to the one equation

$$dW_{\parallel}/dW_{\perp} = -1.2\sqrt{\gamma} k_{\perp}^2 / (k_L k_p), \quad (17)$$

from which we find the upper limit for electron relativistic factor $\gamma_{up} \equiv [k_L k_p / 1.2 k_{\perp}^2]^2$ and the scaling law for the W_{\parallel} (in the lowest order of $1/\gamma_{up}$):

$$\frac{W_{\parallel}}{mc^2} \approx -\frac{2}{3\sqrt{\gamma_{up}}} \gamma^{3/2}, \quad (18)$$

This formula does not depend on the initial conditions (coordinates and momenta of electrons), the wave amplitude and the final energy gain. Despite many approximations, the scaling law (18) describes very well the relation between W_{\parallel} and γ obtained from exact integration

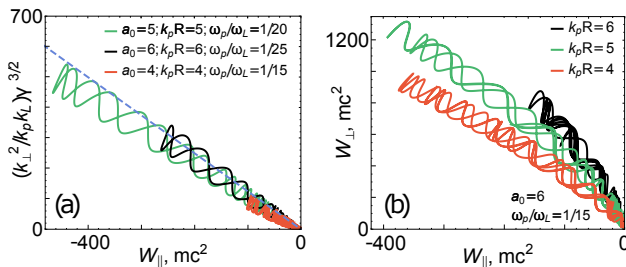


FIG. 3: (a) Relationship between the relativistic factor and the longitudinal work performed by the laser wave at different laser-plasma parameters. Dashed line corresponds to the scaling law (18). (b) Dependence W_{\perp} on W_{\parallel} at different R and the same laser intensity and plasma frequency: the ratio $|W_{\parallel}/W_{\perp}|$ increases with decrease of the channel radius. In all cases, electrons are initially placed at rest on the channel axis at $\phi|_{t=0} = \frac{\pi}{2}$.

of Eqs. (1) - (3) with fields (7) - (9), see Fig. 3(a). Note that $\gamma_{up} \propto k_L^2 k_p^2 R^4$ and therefore a negative role of the longitudinal electric field quickly increases with decrease of the channel radius, see Fig. 3 (b).

Expressions (16) - (15) for transverse and longitudinal work show that the large ratio $E_y^{(L)}/E_x^{(L)}$ is partially counterbalanced for relativistically moving particles by the small ratio $v_y/v_x \sim 1/\sqrt{\gamma}$. This results in moderate difference between W_{\perp} and W_{\parallel} (or γ and W_{\parallel}). Effective acceleration (or deceleration) by the transverse force is accompanied by (de)acceleration (or acceleration) by the longitudinal force. In Appendix, we show that the energy gained by electrons resonantly interacting with the laser pulse confined in the ion channel is always smaller than the energy gained from the planar wave provided that amplitudes and phase velocities are the same.

Since the scaling law (18) is derived by using a very crude approximation for the y -dependence of laser fields, it is not sensitive to specifics of field profiles across the channel. In particular, it can be used for planar channels after replacing $\gamma_{up} \rightarrow [k_L k_p / 1.7 k_{\perp}^2]^2$.

IV. PIC SIMULATIONS

The developed model assumes that accelerating field in the long ion channel is negligibly small. In this section, we design a numerical experiment that clearly the longitudinal laser electric field can significantly change the energy balance of DLA electrons accelerated simultaneously by the laser pulse and the wakefield in the small plasma bubble. The electron dynamics is modeled in realistic 3D geometry using the first-principle self-consistent relativistic 3D PIC code VLPL [31] and quasistatic in-home PIC code (QS-DLA) [32]. The latter can be used as a convenient tool for analyzing the contribution to the electron energy from wake- and laser fields.

We launch two (pump and DLA) laser pulses separated by distance $10\mu\text{m}$ in the tenuous plasma with den-

sity $n_0 = 7.7 \times 10^{18} \text{cm}^{-3}$. The leading pump pulse with the wavelength $\lambda_L = 0.8\mu\text{m}$, power $P = 21\text{TW}$, duration $\tau_{\text{pump}} = 16.6\text{fs}$, spot size $w_{\text{pump}} = 8.7\mu\text{m}$, and dimensionless vector potential $a_0 = 2.9$ blows out electrons on its path creating a plasma bubble. The following DLA pulse with the same wavelength and power, duration $\tau_{\text{DLA}} = 9.4\text{fs}$, spot size $w_{\text{DLA}} = 5.5\mu\text{m}$, and dimensionless vector potential $a_0 = 4.6$ is placed initially near the back of the bubble.

A short electron bunch with duration $\tau_b = 4\text{fs}$, transverse size $3\mu\text{m}$ and small density $n_b = 6.7 \times 10^{15} \text{cm}^{-3}$ is externally injected with initial momentum $p_x = 15mc$ in the $x - y$ plane near the center of the DLA pulse.

The injected electrons co-propagate with the DLA laser pulse simultaneously experiencing acceleration by the laser wave and the bubble wakefield. They approximately reach the bubble center at the dephasing distance $x = 1.15\text{mm}$, see Fig. 4 depicting these electrons and the plasma electron density.

As seen from panels (a) and (b) of this figure, the results of the VLPL and QS-DLA simulations are very similar to each other except for some insignificant differences. Specifically, VLPL simulations reproduce correctly self-injection mechanism [33]. Self-injected electrons are trapped in the plasma bubble during its evolution and localized near the bubble axis behind the cloud of externally injected electrons. The simulations also exhibit some difference in spatial dimensions of the externally injected bunch when it approaches the plasma bubble center. However, in both cases the high energy electrons are positioned at the back of the bunch while the low energy electrons are in bunch front [26].

More detailed characteristics of the injected bunch are presented in Fig. 5. The phase space (W_{\parallel}, W_{\perp}) of particles from VLPL (a) and QS-DLA (b) simulations indicates that the longitudinal work for significant fraction of energetic electrons is negative: $W_{\parallel} = -e \int E_x v_x dt < 0$. If the longitudinal laser electric field were left out of the consideration, one could reach paradoxical conclusion that the wakefield in the plasma bubble decelerates electrons despite the fact that they are positioned in the accelerating phase of the wakefield wave.

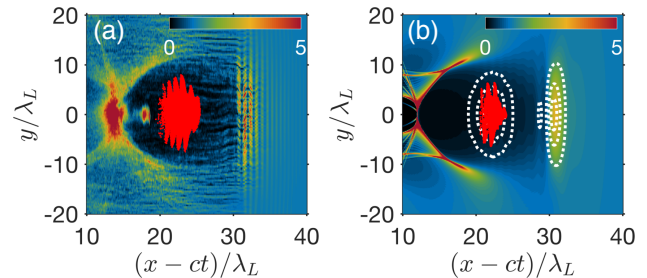


FIG. 4: (a) VLPL and (b) QS-DLA: Plasma bubble at propagation distance $x = 1.15\text{mm}$; externally injected electrons are marked by red points, and pump and DLA pulse contours are plotted with white dashed lines.

In reality, a considerable fraction of the energy gained through the work of the transverse component returns to the laser wave through the negative work of its longitudinal component. This is clarified in Fig. 5(c) and (d): In panel (c) we present the change of W_{\perp} and W_{\parallel} with propagation distance for selected particle in VLPL simulations, and in panel (d) we use advantage of quasistatic code and decompose W_{\parallel} into contributions of the wake and longitudinal laser electric fields. It turns out that in this regime the laser longitudinal component returns to the laser wave approximately half of the energy gained from the work of the transverse component.

In contrast to the model consideration, the conditions of resonant particle-wave interaction in the plasma bubble are constantly changing with time as DLA pulse advances to the bubble center: its amplitude decreases while spot size and the ratio between transverse and longitudinal electric fields increase, see Fig. 6 (a) and (b). Despite that, the ratio between $W_{\parallel}^{(L)}$ and $W_{\perp}^{(L)}$ in Fig. 5(c) is reasonably well described by scaling law (18) if one uses averaged bubble radius $R \approx 10.5\lambda_L$.

Concluding this section, note that in order to accurately reproduce a resonant nature of DLA mechanism by the first principles PIC code, the time step (and the longitudinal cell size) ought to be small. When we decrease resolution of simulations (from $c\Delta t = \lambda/100$ to

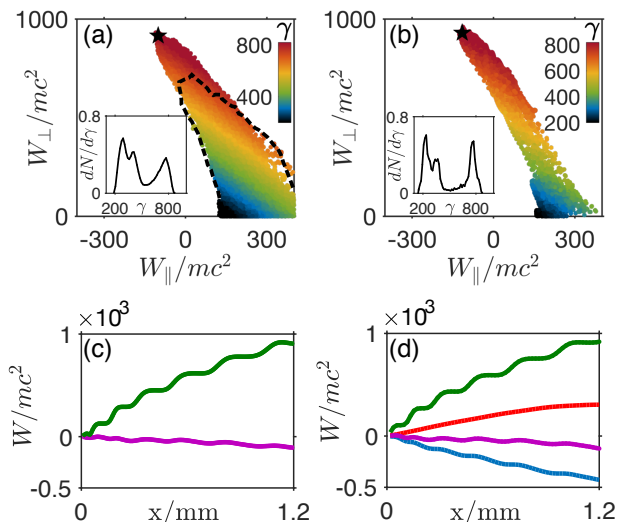


FIG. 5: (a) VLPL and (b) QS-DLA: Phase space (W_{\parallel}, W_{\perp}) of injected electrons color coded by their relativistic factor γ at the propagation distance $x = 1.15mm$. Insets show energy spectrum of these electrons. Dashed black curve in (a) encloses a phase space of particles obtained from VLPL simulations at twice lower resolution ($c\Delta t = \lambda/50$). (c) VLPL and (d) QS-DLA: Transverse W_{\perp} (green) and longitudinal W_{\parallel} (magenta) work as a function of the propagation distance x for the energetic electrons selected by 'black star' in panels (a) and (b). The total longitudinal work W_{\parallel} is decomposed in (d) into the works $W_{\parallel}^{(wake)}$ (red) and $W_{\parallel}^{(L)}$ (blue) done by the wake and the laser, respectively.

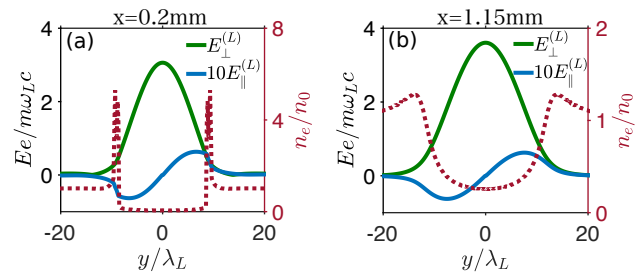


FIG. 6: Dependence of $E_y^{(L)}$ (green), $E_x^{(L)}$ (blue) and $\chi \equiv \langle n_e / \gamma \rangle$ (black) on y at the same propagation distances. Ratio $|E_y^{(L)} / E_x^{(L)}|$ is approximately equal to 45 at $x = 0.2mm$ and 60 at $x = 1.15mm$.

$c\Delta t = \lambda/50$), the electron distribution in the phase space W_{\parallel}, W_{\perp} has changed significantly, see the area inside of the dashed curve in Fig. 5(a).

V. CONCLUSION

We have found that the longitudinal component of the laser electric field can make a profound impact on the energy balance of accelerated (or decelerated) electrons. During resonant direct laser acceleration of particles in ion channels or in plasma bubbles, the transverse and longitudinal components of the laser electric field effectively act in an opposite way: if one component accelerates a particle, the other decelerates it. Since a difference in the field components ($E_x^{(L)} \ll E_y^{(L)}$) is partially counterbalanced by the difference in the velocity components ($v_x \gg v_y$), the corresponding works $W_{\parallel}^{(L)}$ and $W_{\perp}^{(L)}$ can be comparable when DLA pulses propagate in narrow channels or plasma bubbles. The scaling law (18) gives a good estimate for W_{\parallel} and for the upper limit of the electron energy gained through DLA mechanism.

VI. ACKNOWLEDGMENTS

This work was supported by DOE grants de-sc0007889 and de-sc0010622, and by AFOSR grant FA9550-14-1-0045. The authors thank the Texas Advanced Computing Center (TACC) at The University of Texas at Austin for providing HPC resources.

Appendix A: Energy gain from the confined laser pulse propagating in the ion channel

In this Appendix, we show that the energy gained by electrons resonantly interacting with the laser pulse confined in the ion channel is always smaller the energy gained from the planar wave provided that amplitudes and phase velocities are the same.

The confined laser pulse propagates in the ion channel with phase velocity $v_{ph} > c$. This makes analytical consideration quite complicated. However, when $v_{ph} - c \ll c$ ($k_L R_* \gg 1$), equations of motion written in the dimensionless form depend only on two universal parameters \mathcal{E} and χ , which combine laser-plasma properties and electrons initial conditions:

$$\mathcal{E} = a_0(\omega_p/\omega_L)(\tilde{v}_{ph}/c)I_0^{-3/2}, \quad (\text{A1})$$

$$\chi = (I_0/\tilde{v}_{ph}^2)(\tilde{v}_{ph} - 1)/2\omega_p^2/\omega_L^2, \quad (\text{A2})$$

where $\tilde{v}_{ph} = v_{ph}/c$. Using Eq. (11), we can express the parameter χ characterizing superluminality of the wave through the radius of the ion channel:

$$\chi \approx \frac{1.44I_0}{k_p^2 R^2} \quad (\text{A3})$$

We integrate Eqs. (1) - (3) with fields (7) - (9) and find the maximum energy gained by electrons from the confined wave as a function of the \mathcal{E} and $\chi \propto R^{-2}$, see Fig. 7(a). In figure 7(b) and (c) we compare maximum energy gained by electrons from confined and planar wave. The latter is defined as [16]

$$E_y^{(L)} = E_0 \cos \phi, \quad (\text{A4})$$

$$E_x^{(L)} = 0, \quad (\text{A5})$$

$$B_z^{(L)} = \frac{c}{v_{ph}} E_0 \cos \phi. \quad (\text{A6})$$

As expected, the difference between acceleration by the confined and planar wave becomes large as the channel radius decreases (that is, as χ increases).

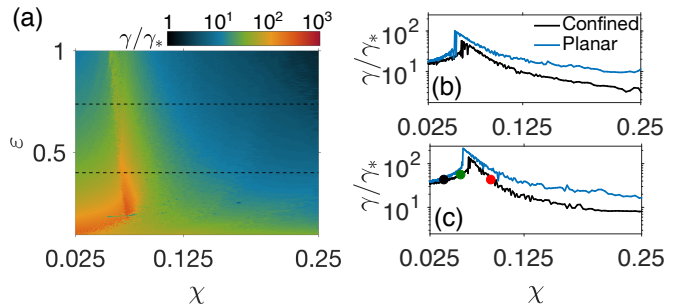


FIG. 7: (a) Maximum energy as a function of the $\mathcal{E} \propto a_0$ and $\chi \propto R^{-2}$; γ is normalized to $\gamma_* = a_0^2/2$, and dashed lines correspond to $\mathcal{E} = 0.74$ and $\mathcal{E} = 0.4$. Electrons are initially placed at rest on the channel axis at $\phi|_{t=0} = \pi/2$. (b) Comparison of the maximum energy gained by electrons from the confined and planar waves along dashed lines in panel (a). Three colored circles (black, green, and red) correspond to three curves (black, green, and red) at the laser-plasma parameters used in Fig. 3.

-
- [1] A. Pukhov, Z.-M. Sheng, J. Meyer-Ter-Vehn, "Particle acceleration in relativistic laser channels," *Phys. Plasmas*, vol. 6, 2847 (1999).
- [2] S. P. D. Mangles, B. R. Walton, M. Tzoufras, Z. Najmudin, R. J. Clarke, A. E. Dangor, R. G. Evans, S. Fritzler, A. Gopal, C. Hernandez-Gomez, W. B. Mori, W. Rozmus, M. Tatarakis, A. G. R. Thomas, F. S. Tsung, M. S. Wei, and K. Krushelnick, "Electron Acceleration in Cavitated Channels Formed by a Petawatt Laser in Low-Density Plasma," *Phys. Rev. Lett.*, vol. 94, 245001 (2005).
- [3] G.V. Stupakov and M. S. Zolotarev, "Ponderomotive Laser Acceleration and Focusing in Vacuum for Generation of Attosecond Electron Bunches," *Phys. Rev. Lett.*, vol. 86, 5274 (2001).
- [4] H.-S. Park, D. M. Chambers, H.-K. Chung, R. J. Clarke, R. Egleton, E. Giraldez, T. Goldsack, R. Heathcote, N. Izumi, M. H. Key, J. A. King, J. A. Koch, O. L. Landen, A. Nikroo, P. K. Patel, D. F. Price, B. A. Remington, H. F. Robey, R. A. Snavely, D. A. Steinman, R. B. Stephens, C. Stoeckl, M. Storm, M. Tabak, W. Theobald, R. P. J. Town, J. E. Wickersham, and B. B. Zhang, "High-energy KK radiography using high-intensity, short-pulse lasers," *Phys. Plasmas*, vol. 13, 056309 (2006).
- [5] S. Kneip, S. R. Nagel, C. Bellei, N. Bourgeois, A. E. Dangor, A. Gopal, R. Heathcote, S. P. D. Mangles, J. R. Marques, A. Maksimchuk, P. M. Nilson, K. Ta Phuoc, S. Reed, M. Tzoufras, F. S. Tsung, L. Willingale, W. B. Mori, A. Rousse, K. Krushelnick, and Z. Najmudin, "Observation of Synchrotron Radiation from Electrons Accelerated in a Petawatt-Laser-Generated Plasma Cavity," *Phys. Rev. Lett.*, vol. 100, 105006 (2008).
- [6] D.J. Stark, T. Toncian, and A.V. Arefiev, "Enhanced Multi-MeV Photon Emission by a Laser-Driven Electron Beam in a Self-Generated Magnetic Field," *Phys. Rev. Lett.*, vol. 116, 185003 (2016).
- [7] M. Schollmeier, A. B. Sefkow, M. Geissel, A. V. Arefiev, K. A. Flippo, S. A. Gaillard, R. P. Johnson, M. W. Kimmel, D. T. Offermann, P. K. Rambo, J. Schwarz, and T. Shimada, "Laser-to-hot-electron conversion limitations in relativistic laser matter interactions due to multipicosecond dynamics," *Phys. Plasmas*, vol. 22, 043116 (2015).
- [8] I. Pomerantz, E. McCary, A. Meadows, A. Arefiev, A. Bernstein, C. Chester, J. Cortez, M. Donovan, G. Dyer, E. Gaul, D. Hamilton, D. Kuk, A. Lestrade, C. Wang, T. Ditmire, and B. Hegelich, "Ultrashort pulsed neutron source," *Phys. Rev. Lett.*, vol. 113, 184801 (2014).
- [9] H. Chen, A. Link, Y. Sentoku, P. Audebert, F. Fiuza, A. Hazi, R. F. Heeter, M. Hill, L. Hobbs, A. J. Kemp, G. E. Kemp, S. Kerr, D. D. Meyerhofer, J. Myatt, S. R. Nagel, J. Park, R. Tommasini, and G. J. Williams, "The scaling of electron and positron generation in intense laser-solid interactions," *Phys. Plasmas*, vol. 22, 056705 (2015).
- [10] A. Pukhov, J. Meyer-Ter-Vehn, "Laser wake field acceleration: the highly non-linear broken-wave regime," *Appl.*

- Phys. B*, vol. 74, 355-361 (2002).
- [11] W. Leemans, B. Nagler, A. Gonsalves, C. Toth, K. Nakamura, C. Geddes, E. Esarey, C. Schroeder and S. Hooker, "GeV electron beams from a centimetre-scale accelerator," *Nat. Phys.*, vol. 2, 696 (2006).
- [12] W. P. Leemans, A. Gonsalves, H. S. Mao, K. Nakamura, C. Benedetti, C. B. Schroeder, C. Toth, J. Daniels D. E. Mittelberger, S. S. Bulanov, J. L. Vay, C. G. R. Geddes, E. Esarey, "Multi-GeV Electron Beams from Capillary-Discharge-Guided Subpetawatt Laser Pulses in the Self-Trapping Regime," *Phys. Rev. Lett.*, vol. 113, 245002 (2014).
- [13] X. Wang, R. Zgadzaj, N. Fazel, Z. Li, S. A. Yi, X. Zhang, W. Henderson, Y. Chang, R. Korzekwa, H. Tsai, C.-H. Pai, H. Quevedo, G. Dyer, E. Gaul, M. Martinez, A. C. Bernstein, T. Borger, M. Spinks, M. Donovan, V. Khudik, G. Shvets, T. Ditmire and M. C. Downer, "Quasi-monoenergetic laser-plasma acceleration of electrons to 2 GeV," *Nat. Commun.*, vol. 4, 1998 (2013).
- [14] H. T. Kim, K. H. Pae, H. J. Cha, I. J. Kim, T. J. Yu, J. H. Sung, S. K. Lee, T. M. Jeong, and J. Lee, "Enhancement of Electron Energy to the Multi-GeV Regime by a Dual-Stage Laser-Wakefield Accelerator Pumped by Petawatt Laser Pulses," *Phys. Rev. Lett.*, vol. 111, 165002 (2013).
- [15] C Gahn, G D Tsakiris , A Pukhov, J Meyer-ter-Vehn, G Pretzler, P Thirolf, D Habs, K J Witte, "Multi-MeV Electron Beam Generation by Direct Laser Acceleration in High-Density Plasma Channels," *Phys. Rev. Lett.*, vol. 83, 23 (1999).
- [16] V. N. Khudik, Xi Zhang, T. Wang, and G. Shvets, "Far-field constant-gradient laser accelerator of electrons in an ion channel," *Phys. Plasmas*, vol. 25, 083101 (2018).
- [17] J. L. Shaw, F. S. Tsung, N. Vafaei-Najafabadi, K. A. Marsh, N. Lemos, W. B. Mori and C. Joshi, "Role of direct laser acceleration in energy gained by electrons in a laser wakefield accelerator with ionization injection," *Plasma Phys. Control. Fusion*, vol. 56, 084006 (2014).
- [18] Y. Zhang and S. I. Krasheninnikov, "Electron dynamics in the laser and quasi-static electric and magnetic fields," *Physics Letters A* vol. 382.27, 1801 (2018).
- [19] A. V. Arefiev, B. N. Breizman, M. Schollmeier, and V. N. Khudik, "Parametric amplification of laser-driven electron acceleration in underdense plasma," *Phys. Rev. Lett.*, vol. 108, 145004 (2012).
- [20] A. V. Arefiev, V. N. Khudik, and M. Schollmeier, "Enhancement of laser-driven electron acceleration in an ion channel," *Phys. Plasmas*, vol. 21, 033104 (2014).
- [21] A. V. Arefiev, V. N. Khudik, A. P. L. Robinson, G. Shvets, and L. Willingale, "Spontaneous emergence of non-planar electron orbits during direct laser acceleration by a linearly polarized laser pulse," *Phys. Plasmas*, vol. 23, 023111 (2016).
- [22] T. W. Huang, C. T. Zhou, A. P. L. Robinson, B. Qiao, A. V. Arefiev, P. A. Norreys, X. T. He, and S. C. Ruan, "Nonlinear parametric resonance of relativistic electrons with a linearly polarized laser pulse in a plasma channel," *Phys. Plasmas*, vol. 24, 043105 (2017).
- [23] V. N. Khudik, A. V. Arefiev, X. Zhang and G. Shvets, "Universal scalings for laser acceleration of electrons in ion channels," *Phys. Plasmas*, vol. 23, 103108 (2016).
- [24] A. Robinson, A. Arefiev, V. Khudik, "The effect of superluminal phase velocity on electron acceleration in a powerful electromagnetic wave," *Phys. Plasmas*, vol. 22, 083114 (2015).
- [25] X. Zhang, V. N. Khudik, and G. Shvets, "Synergistic Laser-Wakefield and Direct-Laser Acceleration in the Plasma-Bubble Regime," *Phys. Rev. Lett.* vol. 114, 184801 (2015).
- [26] X. Zhang, V. N. Khudik, A. Pukhov and G. Shvets, "Laser wakefield and direct acceleration with ionization injection," *Plasma Phys. Control. Fusion*, vol. 58, 034011 (2016).
- [27] X. Zhang, T. Wang, V. N. Khudik, A. C. Bernstein, M. C. Downer, and G. Shvets, "Effects of laser polarization and wavelength on hybrid laser wakefield and direct acceleration", *Plasma Phys. Control. Fusion*, vol. 60, 105002 (2018).
- [28] N. Naseri, S. G. Bochkarev, and W. Rozmus, "Self-channelling of relativistic laser pulses in large-scale underdense plasmas," *Phys. Plasmas*, vol. 17, 033107 (2010).
- [29] K. Okamoto, "Fundamentals of Optical Waveguides," (Academic, San Diego, 2006).
- [30] X. Davoine, F. Fiza, R. A. Fonseca, W. B. Mori, L. O. Silva, "Beam quality requirements for the Ion-Channel Laser," arXiv:1404.7373 (2014).
- [31] A. Pukhov, "Three-dimensional electromagnetic relativistic particle-in-cell code VLPL (Virtual Laser Plasma Lab)", *J. Plasma Phys.*, vol. 61, 425 (1999).
- [32] T. Wang, V. Khudik, B. Breizman, and G. Shvets, "Non-linear plasma waves driven by short ultrarelativistic electron bunches", *Phys. Plasmas*, vol. 24, 103117 (2017).
- [33] S. Kalmykov, S. A. Yi, V. Khudik, and G. Shvets, "Electron Self-Injection and Trapping into an Evolving Plasma Bubble," *Phys. Rev. Lett.*, vol. 103, 135004 (2009).